Hindawi
Journal of Nanomaterials
Volume 2023, Article ID 7036247, 9 pages
https://doi.org/10.1155/2023/7036247

Research Article

Green Synthesis Method of ZnO Nanoparticles using Extracts of *Zingiber officinale* and Garlic Bulb (*Allium sativum*) and Their Synergetic Effect for Antibacterial Activities

Solomon Kebede Urge, Solomon Tiruneh Dibaba, and Abebe Belay Gemta

Department of Applied Physics, School of Applied Natural Science, Adama Science and Technology University, P.O. Box 1888, Adama, Ethiopia

Correspondence should be addressed to Solomon Tiruneh Dibaba; solomondibaba27@gmail.com

Received 29 August 2022; Revised 26 November 2022; Accepted 29 November 2022; Published 12 January 2023

Academic Editor: Vidya Nand Singh

In this paper, antibacterial activities of zinc oxide (ZnO) nanoparticles synthesized through green method using garlic bulb (*Allium sativum*), ginger (*Zingiber officinale*) extracts, and their mixture are reported. The synthesized ZnO NPs were characterized by X-ray diffraction (XRD), ultraviolet visible (UV–vis), photoluminescence (PL), spectroscopy and Fourier transform infrared (FTIR) spectroscopy. The crystalline sizes of ZnO NPs synthesized using garlic bulb (*Allium sativum*) extract, ginger (*Zingiber officinale*) root extract, and their mixture were 19.8, 21.94, and 23.86 nm, respectively. Similarly, the corresponding peak absorbances were 369.5, 377.5, and 374 nm, respectively. The antibacterial activities of synthesized ZnO NPs were tested against gram-negative bacteria *Escherichia coli* (*E. coli*) and *Pseudomonas putida* (*P. putida*) and gram-positive bacteria *Staphylococcus aureus* (*S. aureus*) and *Streptococcus pyogenes* (*S. pyogenes*). The ZnO NPs synthesized using the mixture of garlic bulb (*Allium sativum*) and ginger (*Z. officinale*) root extract have shown maximum inhibition zone against gram-negative bacteria (*P. putida*: 28.67 ± 0.82 mm) and gram-positive bacteria (*S. pyogenes*: 10.67 ± 0.47 mm) as compared to ZnO NPs synthesized using the two extracts separately. On the other hand, ZnO NPs obtained from garlic bulb and *Z. officinale* root extracts exhibited maximum inhibition zone against *E. coli* (19 ± 0.82 mm) and *S. aureus* (16.4 ± 0.47 mm), respectively.

1. Introduction

The novel properties of nanomaterials bring the rapid development of nanoscience and nanotechnology. Among nanomaterials, metal oxide nanoparticles received exceedingly attention from the scientific community because of their size-tunable several unique properties, such as high chemical stability, high electrochemical coupling coefficient, broad range of radiation absorption, high photostability, easily availability, low cost, and nontoxicity [1–7].

Among metal oxide nanomaterials, zinc oxide (ZnO) nanoparticle is one of the foremost considered metal oxide nanomaterials due to its unique chemical, physical, biological, and optical properties [8–10]. ZnO NPs have many applications in different fields like, optical, piezoelectric, mechanical, biomedical, gas sensing, catalyst, etc. [11, 12].

There are different methods of synthesizing ZnO NPs, including hydrothermal [13], sol−gel processing [14], spray pyrolysis method [15], coprecipitation [16], chemical vapor deposition (CVD) [17], green synthesis method, etc. Among these synthesis methods, green synthesis using plant extracts is commonly preferred for the synthesis of ZnO NPs due to eco-friendly, cost-effective, and nontoxicity of the resulting NPs for human therapeutic use [18].

Green synthesis of ZnO NPs has been carried out by extracting different plants such as *Cassia fistula* and *Melia Azadarch* [19], garlic (*Allium sativum*) [20], *Z. officinale* (ginger), *Aloe vera* [21], coffee [22], orange peel extract [23], *Cardamom* [24], and *Lippia adoensis* (*koseret*) [25]. However, the comparison of antimicrobial activities of ZnO synthesized using ginger (*Z. officinale*), garlic (*Allium sativum*) extract, and most importantly the antimicrobial activities of ZnO

nanoparticles synthesized by the synergetic effect of the mixture of the two extracts were not performed so far to the best of our knowledge. This study was conducted to compare antibacterial activities of ZnO NPs synthesized using *Z. officinale* root extract, garlic bulb (*Allium sativum*) extract, and their mixture against the two standard pathogens, gram-positive and gram-negative bacteria.

Ginger is the most frequently and heavily consumed dietary condiments in the world. Ginger is frequently prescribed by Indian and Chinese medicine for the treatment of cough, common cold, rheumatism, snake bite, and respiratory problems [26]. It is also used in treatment of cancer, skin diseases, heart palpitation, swelling, urinary problems, stomach problems, abdomen problems, dyspepsia, and loss of appetite [27]. Chemically, ginger is rich in flavonoids and polyphenolic compounds such as gingerols, shagols, zingerone, paradol, terphineol, terpenes, borneol, geraniol, limonene, linalool, and alpha-zingiberene [28].

Similarly, garlic is used worldwide as a food additive, spice, and medicine. It has been described as a gastric stimulant. Garlic (*Allium sativum*) is a rich source of organosulfur compounds showing a variety of biological activities [29] such as, allyl sulfide, allicin, allyl cysteine, ajoene, and alliin [30]. Phenols, terpenoids, ketones, aldehydes, and amides in plants were responsible for the production of metal NPs [31].

2. Experimental Method

2.1. Materials and Chemicals. The materials used for the synthesis were contained: fresh root of ginger (*Z. officinale*), garlic bulb (*Allium sativum*), beaker, magnetic stirrer, hot plate, incubator, power supply, thermometer, Whatman No. 1 filter papers, digital electronic analytical balance (Model FA2104, China), furnace (Model BK-5-12GJ), ceramic crucible cups, drying oven (Model 101-0, Biobase Biodustry, Shandong Co. Ltd, China), cylinders, and centrifuge (Model AVI-558, max RPM:5,000 rpm).

The precursor chemicals used for the synthesis were included: zinc acetate ($Zn(CH_3COO)_2{\cdot}2H_2O$) (molar: 219.49 g/mol, Merk Life Science, PLC), deionized water, ethanol, sodium hydroxide (NaOH), dimethyl sulfoxide (DMSO, $(CH_3)_2OS$, 99.9% pure, Loba Chemie Pvt. Ltd., India), zinc acetate dehydrate was provided as precursors and sodium hydroxide was used for controlling the pH values. All the reagents used in the experiments will be in analytical grade and used without any further purification.

2.2. Methods of Extraction. The fresh root of *Z. officinale* and garlic was purchased from local market (Adama, Ethiopia). *Z. officinale* sample was washed thoroughly and soaked in distilled water for 20 min in order to remove dirty present on the skin of sample. In the same manner, garlic was washed using distilled water after the outer skin was pilled off. The roots were completely air-dried and the moisture contents were removed. The dried roots were crushed using mortar and pestle. After that, 10 g of the powder of each sample was boiled for 30 min in 100 mL of deionized water (DW). Finally, the extracts were filtered with the Whatman No. 1 filter paper and stored at 4°C for further use. These steps are indicated in Figures 1–3.

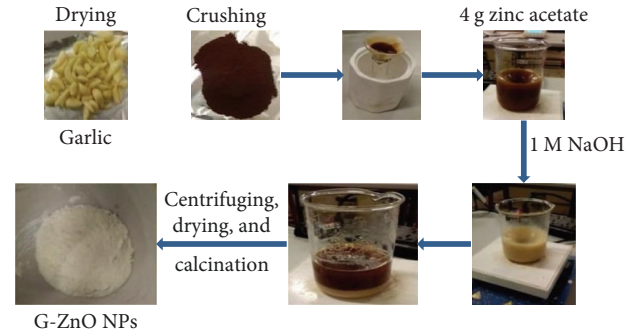

Figure 1: Schematics of ZnO NPs synthesized using garlic bulb extract.

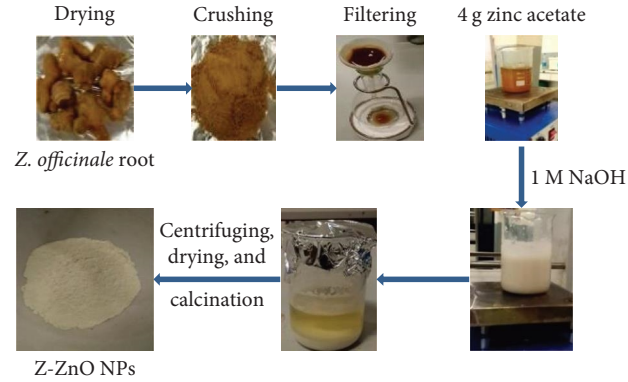

Figure 2: Schematic of ZnO NPs synthesized using *Z. officinale* root extract.

2.3. Synthesis of ZnO NPs. Four grams of zinc acetate ($Zn(CH_3COO)_2{\cdot}2H_2O$) was added into 50 mL of deionized water (DW) to get final concentration of zinc acetate dehydrate ($Zn(C_2H_3O_2)_2{\cdot}2H_2O$). Ten milliliters of *Z. officinale* root extract and garlic bulb extract were slowly added to zinc acetate dehydrate solution in the different beaker and 10 mL of their mixtures were added to zinc acetate dehydrate solution in the same ratio. 1 M of NaOH were added drop-by-drop to the solution to control the pH of the solutionat 12 [32, 33]. The mixtures were heated and stirred on magnetic stirrer for 2 hr at 50°C until the white precipitate was observed. Then, the pellets were centrifuged three times for 10 min interval at 5,000 rpm and dried in an oven overnight. Then, the dried samples were calcined in a muffle furnace at 450°C for 2 hr and the powders were collected for characterization. Figures 1–3 represent the schematics of synthesized ZnO NPs using garlic bulb extract, *Z. officinale* root extract, and their mixture, respectively.

2.4. Characterization Techniques. Some of the instruments used for characterization of ZnO NPs were X-ray diffraction (XRD) (X-ray target tube, Cu–Kα radiation, 40 kV, scanning rate 3° min^{-1}, recorded 2θ range between 10° and 80°) used to study the crystal structure the nanoparticles, UV–visible

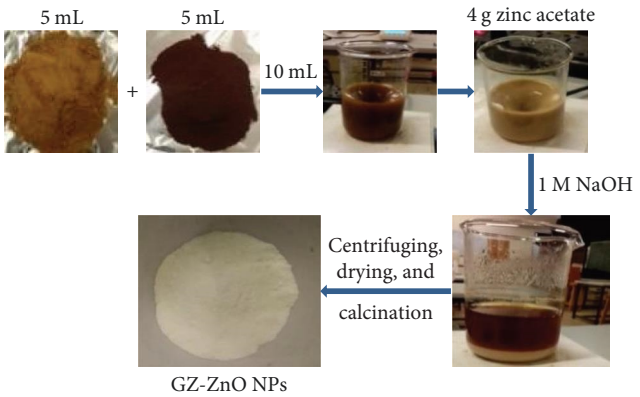

FIGURE 3: Schematic of ZnO NPs synthesized using the mixture of *Z. officinale* root and garlic bulb extract.

spectroscopy (UV-3600Plus series) to measure energy band-gap of the particles, photoluminescence (PL) spectroscopy (Cary Eclipse fluorescence spectrophotometer, scan rate 600 nm/min, MY18490002, Agilent Technologies, Malaysia) to determine the emission spectra of the nanoparticles and FTIR spectroscopy (IS50, APX, Germany) to characterize the functional groups attached to synthesized ZnO nanoparticles.

2.5. Antibacterial Activities. The antibacterial activities of ZnO NPs were tested against standard pathogens of gram negative (*E. coli*-ATCC 9637 and *P. putida*-ATCC 47054) and gram positive (*S. aureus*-ATCC 6538 and *S. pyogenes*-ATCC 19615) by agar well diffusion method (at concentration about 5×10^5 CFU/mL). Ampicillin was used as positive control in each plate. The plates were incubated for 18 hr at 37°C. The stock solution of synthesized ZnO NPs was prepared in dimethyl sulfoxide (DMSO, $(CH_3)_2OS$, 99.9% pure, Loba Chemie Pvt. Ltd., India) at different concentrations: 15, 10, and 5 mg/mL.

3. Results and Discussion

3.1. XRD Analysis. X-ray diffraction patterns of synthesized ZnO NPs peaks were agreed with the ordinary data (JCPDS card no. 00-036-1451). Figure 4 shows the characteristic Bragg diffraction at 2θ values of the three samples. The first sample is ZnO NPs synthesized using *Z. officinale* root extract (Z-ZnO NPs: Figure 4(a)) shows the distinctive Bragg diffraction at 2θ values of 31.22, 31.78, 34.07, 34.44, 36.26, 36.93, 44.02, 47.55, 56.61, 62.28, 62.87, 64.38, 66.39, 67.96, 69.09, 76.95, and 77.46. The strongest peaks are $2\theta = 36.26$, 31.78, and 34.44. The second one is ZnO NPs synthesized using garlic extract (G-ZnO NPs: Figure 4(b)) indicates the distinctive Bragg diffraction at 2θ values of 31.76, 34.42, 36.24, 47.53, 56.02, 56.58, 62.86, 66.39, 67.95, 69.04, and 77.09. The strongest peaks are three peaks observed at $2\theta = 36.24$, 34.42, and 31.76. The third one is ZnO NPs synthesized using the mixture of *Z. officinale* root extract and garlic extract (GZ-ZnO NPs: Figure 4(c)) shows the distinctive Bragg diffraction at 2θ values of 31.79, 33.91, 34.45, 36.27, 36.85, 47.56, 56.06, 56.62, 57.18, 62.42, 62.88, 66.41, 67.97, and 69.09. The strongest peaks are $2\theta = 34.44$, 31.22,

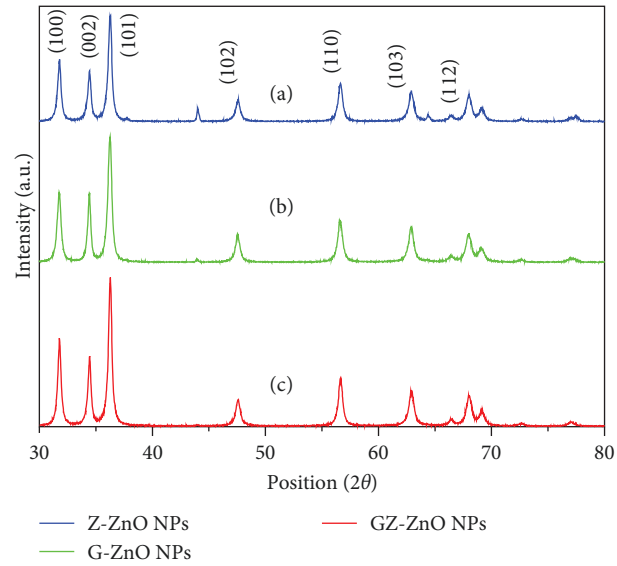

FIGURE 4: XRD patterns of ZnO NPs synthesized using: (a) *Z. officinale* root extract; (b) garlic bulb extract; (c) the mixture of *Z. officinale* root and garlic bulb extract.

and 34.07. They were indexed to the plane (100), (002), (101), (102), (110), (103), (200), (112), and (201) that are in good agreement with wurtzite ZnO structure. The distinct and clear peaks confirmed the high purity and crystalline nature of the prepared ZnO NPs. The crystallite size has been estimated from the broad diffraction peak using the Debye–Scherrer formula.

$$D_p = \frac{0.9\lambda}{\beta \cos\theta}, \quad (1)$$

where D is the crystal size of ZnO NPs, k is Scherrer's constant given by 0.9, λ is the wavelength of X-rays (1.541 Å), θ is the Bragg diffraction angle, and β is the full-width at half-maximum (FWHM) of the diffraction peak corresponding to plane (101). The average particle size of ZnO NPs synthesized using garlic bulb (*Allium sativum*) extract, *Z. officinale* (ginger) root extract, and their mixture were found to be 19.8, 21.94, and 23.86 nm, which were derived from the FWHM of the more intense peak ($\beta = 0.422$, 0.380, 0.350) corresponding to the (101) plane located at $2\theta = 36.24°$, 36.26°, and 36.27°, respectively.

The average particle size of synthesized ZnO NPs obtained from XRD data shows good results compared to the previous report [34]. Vidya et al. [10] synthesized ZnO NPs by using *Calotropis gigantea* and reported the average grain size as 30–35 nm. Yuvakkumar et al. [35] synthesized ZnO NPs using noble plant rambutan (*Nephelium lappaceum* L) peel extract and has reported the average crystalline size as 50.95 nm.

3.2. Photoluminescence (PL) Spectrum. Figure 5 indicates the PL spectrum (peak emission) of ZnO NPs synthesized using *Z. officinale* root extract, garlic extract, and their mixture. A broad blue emission peak centered at (421.05 nm), (393 and

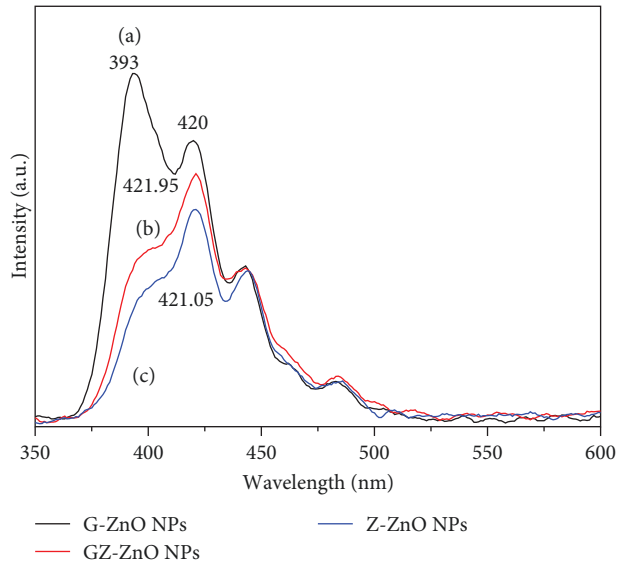

Figure 5: The emission spectra of ZnO NPs synthesized using: (a) garlic bulb (G) extract; (b) the mixture of garlic bulb and *Z. officinale* root extract (GZ); (c) *Z. officinale* (*Z*) root extract at excitation wavelength of 325 nm.

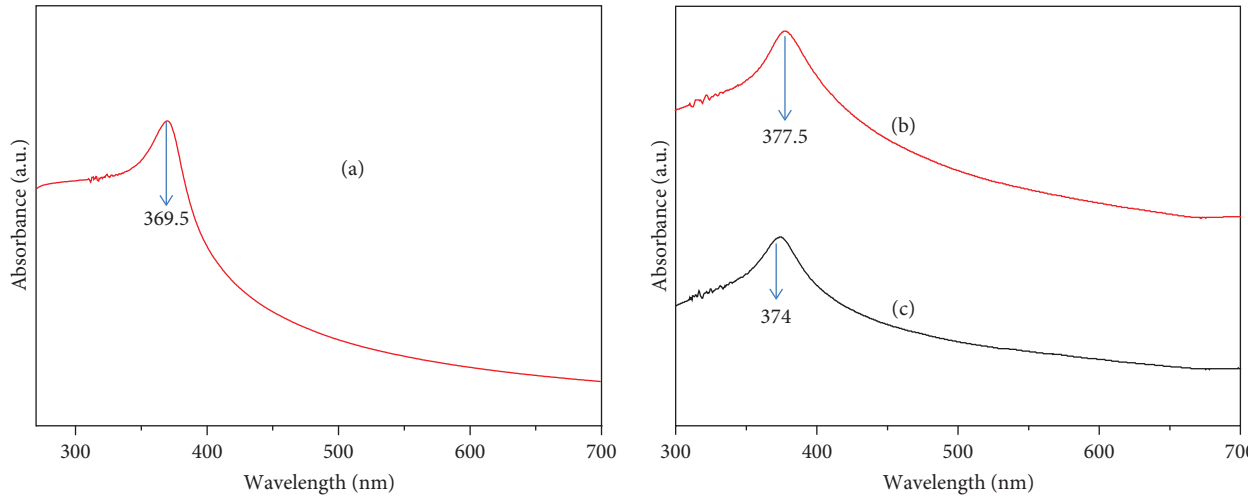

Figure 6: UV–vis absorbance spectra of ZnO NPs synthesized using: (a) garlic bulb extract; (b) *Z. officinale* root extract; (c) the mixture of garlic bulb and *Z. officinale* root extract.

420 nm), and (421.95 nm) can be observed for ZnO NPs synthesized using *Z. officinale* root extract, garlic extract, and their mixtures, respectively. From the evidence of given data (Figure 5), the different peaks exists at different wavelength, which were normally associated with Zn defects, such as transitions of an electron from conduction band to the valance band and O_2 vacancies [36]. The O_2 vacancies change the properties of oxide materials by producing F centers of ionic oxides which may cause the formation of metal–metal bonds in covalent bond. In other case, O_2 vacancies change the oxidation state of compounds of transition metal atoms with empty d orbitals, which can eventually alter the local electronic structure of atoms [37]. In n-type ZnO, acceptor-like defects (O_i) are easier to form, which enables the transition between different bandgap energies [38]. The PL emission rate is directly proportional to the photo-excited load carrier's recombination probability. Higher PL strength advanced e^-/h^+ pair (electron–hole pair) recombination and guides to the lower photocatalytic activity [39].

3.3. UV–Vis Absorbance. Figure 6 shows the UV–vis absorbance of ZnO NPs synthesized by using *Z. officinale* root extract, garlic extract, and their mixture. The optical bandgap energy of ZnO NPs synthesized using *Z. officinale* root extract, garlic bulb extract, and their mixture calculated using Tauc formula was found to be 3.2, 3.27 and 3.24 eV at maximum wavelength of 377.5, 369.5, and 374 nm, respectively.

The calculated bandgap energy (E_g) of synthesized ZnO NPs were performed in good agreement with the optical bandgap energy of standard ZnO NPs.

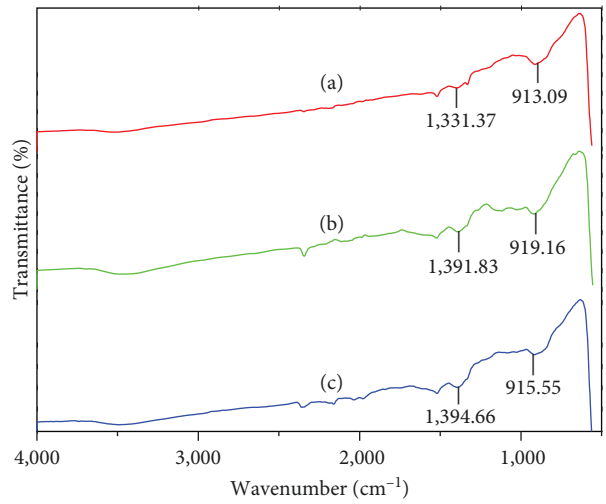

Figure 7: FTIR spectra of ZnO NPs synthesized using: (a) garlic bulb extract; (b) *Z. officinale* root extract; (c) the mixture of garlic bulb and *Z. officinale* root extract respectively.

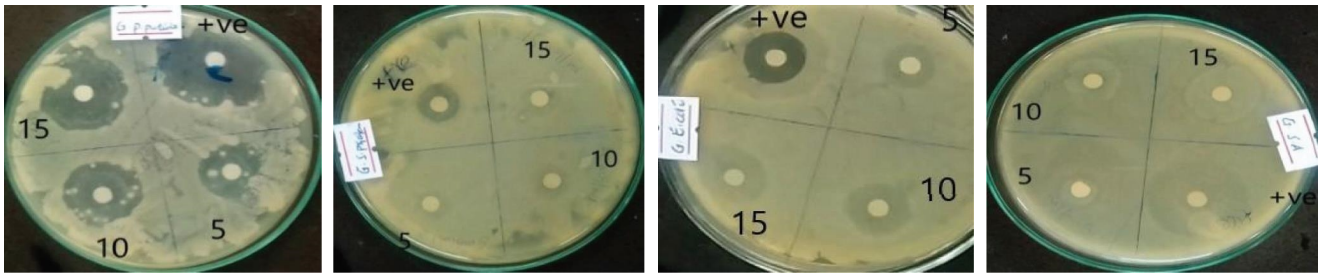

Figure 8: Antimicrobial activities of ZnO NPs synthesized using garlic bulb extract against *E. coli*, *P. putida*, *S. pyogenes*, and *S. aureus*, respectively.

To evaluate the energy band gap we used the Tauc equation:

$$(\alpha h\nu)^{\gamma} = A\left(h\nu - E_g\right), \tag{2}$$

where E_g is energy bandgap, h is Planks constant, α is absorption coefficient, ν is the frequency given by ($\nu = c/\lambda$), γ is the nature of electronic transition which equal to 1/2 for direct bandgap, and A is constant, usually taken as 1 for amorphous materials [40].

3.4. FTIR Analysis. FTIR spectroscopy was performed to identify the functional groups associated with the ZnO NPs formation. Figure 7(a)–7(c) represents the FTIR spectrum of ZnO NPs synthesized using garlic bulb extract, *Z. officinale* root extract, and their mixture, respectively. ZnO NPs absorption band was obtained within the region 4,000–400 cm^{-1}. The bands at 913.09, 919.16, and 915.55 cm^{-1} in FTIR spectrum confirm the C–H bending of alkenes in ZnO NPs synthesized using garlic bulb extract, *Z. officinale* root extract, and their mixtures, respectively [41]. The bands that are near to 1,000 cm^{-1} are associated with metal−oxygen tension and bending, in this case, Zn–O bonding was formed [42]. Broadband at 3,400–3,200 cm^{-1} showed characteristic OH group. Bands at 1,331.37, 1,391.83, and 1,394.66 cm^{-1} confirmed the presence of carboxylic acid and aromatic C–H bending [43]. Therefore, the present studies agreed with the previous report.

3.5. Antibacterial Activities. The bactericidal activities of ZnO NPs synthesiszed using garlic bulb extract, *Z. officinale* root extract, and their mixtures were tested against standard pathogenes gram-negative (G–ve) and gram-positive (G+ve) bacteria. From G–ve, *Escherichia coli* (*E. coli*) and *Pseudomonas putida* (*P. putida*) and from G+ve, *Staphylococcus aureus* (*S. aureus*), and *Streptococcus pyogenes* (*S. pyogenes*) were grown to test the antimicrobial activities of synthesized ZnO NPs. Figures 8–10 show zone of inhibition of the four bacteria against synthesized ZnO NPs at the concentration of 15, 10 and 5 mg/mL. The mean values of zone of inhibition of three replicates are shown in Tables 1–3. As the concentration of synthesized NPs increased, the zone of inhibition also increased. The small particle size and the high surface area of ZnO NPs can increase antimicrobial activity, causing an improvement in surface reactivity [44].

Garlic-mediated ZnO NPs were more significant on G–ve bacteria *P. putida* (21.67 ± 0.88 mm) and *E. coli* (19 ± 0.82 mm) compared to G+ve bacteria *S. aureus* (17.7 ± 0.47 mm) and *S. pyogenes* (7 ± 0.82 mm) as shown in Figure 8 and Table 1.

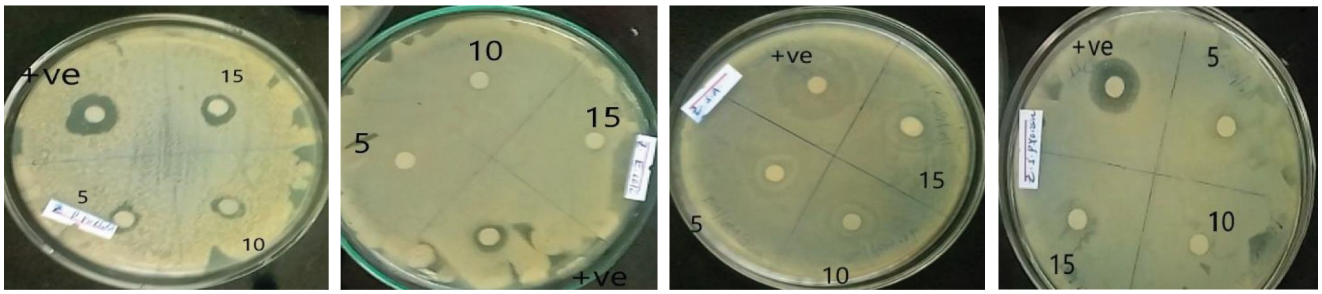

Figure 9: Antimicrobial activities of ZnO NPs synthesized using *Z. officinale* root extract against *P. putida, E. coli, S. aureus*, and *S. pyogenes*, respectively.

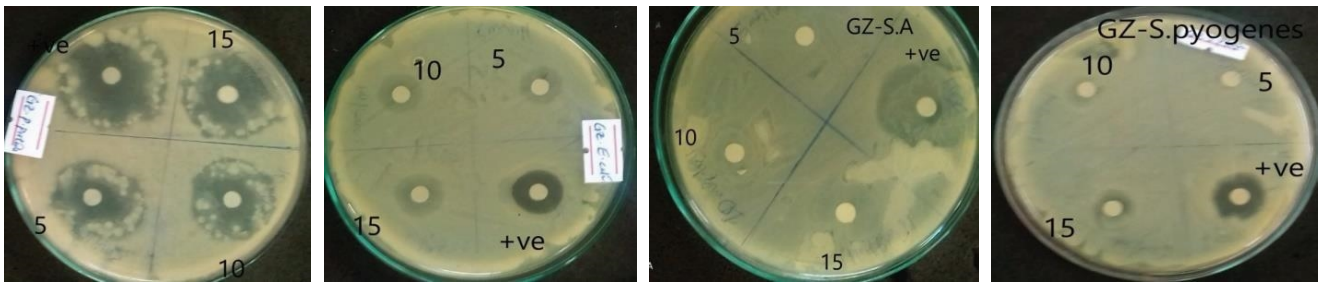

Figure 10: Antimicrobial activities of ZnO NPs synthesized using the mixture of garlic bulb extract and *Z. officinale* root extract against *P. putida*, *E. coli*, *S. aureus*, and *S. pyogenes*, respectively.

Table 1: Antibacterial activities of ZnO NPs synthesized using garlic bulb (G) extract at different concentration and their corresponding zone of inhibition (mm).

Bacterial species	Zone of inhibition (mm)			
	G-ZnO NPs			Positive control
	5 mg/mL	10 mg/mL	15 mg/mL	
P. putida	18.67 ± 0.88	21 ± 1.41	21.67 ± 0.88	24.7 ± 0.94
S. aureus	11.7 ± 1.24	13.4 ± 0.47	17.7 ± 0.47	24 ± 0.82
P. pyogenes	5 ± 0.82	6.7 ± 0.47	7 ± 0.82	11.4 ± 0.58
E. coli	11.67 ± 1.24	13.67 ± 0.47	19 ± 0.82	19.3 ± 1.89

Table 2: Antibacterial activities of ZnO NPs synthesized using *Z. officinale* root (Z) extract at different concentration and their corresponding zone of inhibition (mm).

Bacterial species	Zone of inhibition (mm)			
	Z-ZnO NPs			Positive control
	5 mg/mL	10 mg/mL	15 mg/mL	
P. putida	6 ± 0.82	6.4 ± 0.48	7.7 ± 0.78	9 ± 0.00
S. aureus	10 ± 0.82	14.4 ± 0.47	16.4 ± 0.47	19 ± 1.63
P. pyogenes	5 ± 2.16	6 ± 0.57	10 ± 0.82	14.7 ± 0.94
E. coli	2 ± 0.00	2.7 ± 0.78	4 ± 1.00	9 ± 0.00

ZnO NPs synthesized using *Z. officinale* root extract were more effective on G+ve bacteria *S. aureus* (16.4 ± 0.47 mm) and *S. pyogenes* (10 ± 0.82 mm) compared to G−ve bacteria *P. putida* (7.7 ± 0.78 mm) and *E. coli* (4 ± 1.00 mm) as shown in Figure 9 and Table 2. However, it is possible to say that the zone of inhibition of the mixture of garlic bulb and *Z. officinale* (GZ)-mediated ZnO NPs was greater than that of garlic (G)-mediated ZnO NPs and *Z. officinale* root extract (Z)-mediated ZnO NPs against G−ve bacteria like *P. putida*. These results suggest that the use of ZnO NPs synthesized using the mixture of garlic bulb (*Allium sativum*) and *Z. officinale* root extract can be more efficient against gram-negative

Table 3: Antibacterial activities of ZnO NPs synthesized using mixture of garlic bulb and *Z. officinale* root extract (GZ) at different concentration and their corresponding zone of inhibition (mm).

Bacterial species	Zone of inhibition (mm)			
	GZ-ZnO NPs			Positive control
	5 mg/mL	10 mg/mL	15 mg/mL	
P. putida	24 ± 0.82	24.7 ± 0.94	28.67 ± 0.82	29 ± 1.63
S. aureus	9 ± 0.82	11 ± 0.82	15.67 ± 0.82	21.3 ± 1.24
P. pyogenes	7.4 ± 0.94	9 ± 0.82	10.67 ± 0.47	14.7 ± 0.47
E. coli	12.3 ± 1.7	13 ± 0.82	15.3 ± 0.94	17 ± 1.63

Table 4: Comparing zone of inhibition of synthesized ZnO NPs synthesized using green methods with the previously reported references.

Bacterial species	Zone of inhibition (mm)	References
E. coli	18 ± 6	[35]
E. coli	2–3	[34]
E. coli	15.00 ± 0.00 mm	[46]
E. coli	19 ± 0.82	This study
P. putida	28.67 ± 0.82	This study

bacteria (G−ve). This might be due to the presence of higher number of phenolic compounds and rare secondary metabolites present in both garlic and *Z. officinale*. Dobrucka and Długaszewska [45] reported that reactive oxygen species (ROS) such as superoxide and hydroxyl radicals produced by ZnO NPs were caused damage to bacterial cell membranes.

According to the evidence of zone of inhibition of the recorded data shown in Figure 10 and Table 3, ZnO NPs synthesized using the mixtures of garlic bulb and *Z. officinale* root extract (GZ) was more effective on the G−ve bacteria *P. putida* (28.67 ± 0.82 mm) and *E. coli* (15.3 ± 0.94 mm) compared to G+ve bacteria *S. pyogenes* (10.67 ± 0.47 mm) and *S. aureus* (15.67 ± 0.82 mm).

In general, ZnO NPs synthesized using the mixtures of garlic bulb and *Z. officinale* root extract (GZ) showed the highest inhibition zone, this is maybe due to interaction of ZnO NPs with cell membrane of the bacteria (*E. coli*, *P. putida*, *S. pyogenes*, and *S. aureus*). The ZnO particles entered into the bacterial cell creates reactive oxygen species (ROS) that react with cysteinyl protein and iron inside the cells and cause DNA and cell wall damage. Besides, the garlic bulb (*Allium sativum*) extract and *Zingiber officinale* (ginger) root extract that were used as reducing agent have phytochemicals that are toxic to bacteria. As a result the synergetic effect enhances inhibition zones of the bacteria. The comparison of our results with some previously reported results is shown in Table 4.

4. Conclusion

In this work, ZnO NPs using *Z. officinale* root extract, garlic bulb extract, and their mixture were successfully synthesized. The XRD examinations of synthesized ZnO NPs were confirmed the formation of wurtzite shape NPs. The absorption spectra of ZnO NPs synthesized using garlic bulb extract, *Z. officinale* root extract, and their mixture were found to be 369.5, 377.5, and 374 nm, respectively. The bands at 913.09, 919.16, and 915.55 cm^{-1} in FTIR spectrum confirms the formation of ZnO NPs and the PL spectrum centered at 421.06, 421.96 and 421.95 nm shows the peak emission of ZnO NPs synthesized using garlic bulb extract, *Z. officinale* root extract, and their mixture, respectively. According to the evidence shown in Figure 10 and Table 3, we observed that ZnO NPs synthesized using the mixture of garlic bulb and *Z. officinale* root extract, reported for the first time, exhibited high inhibition zone against gram-negative bacteria, *P. putida* ($28.67 \pm .0.82$). This might be due to ROS generated by the ZnO nanoparticles entered to the bacteria cell and the presence of higher number of phenolic compounds and rare secondary metabolites present in both garlic bulb and *Z. officinale* root. Further study may be needed to utilize this kind of synergistic green synthesis methods for antifungal and anticancer application in the future.

Data Availability

All the necessary data are already included in the main manuscript.

Conflicts of Interest

The authors declare that they have no conflicts of interest.

Acknowledgments

This work is financially supported by the Adama Science and Technology University.

References

[1] W.-T. Liu, "Nanoparticles and their biological and environmental applications," *Journal of Bioscience and Bioengineering*, vol. 102, no. 1, pp. 1–7, 2006.

[2] C. P. Poole, Jr. and F. J. Owens, *Introduction to Nanotechnology*, John Wiley Sons, Inc., 2003.

[3] S. Hussain, "*Investigation of structural and optical properties of nanocrystalline ZnO*," Thesis Report, The Department of Physics, Chemistry and Biology, Linköpings University, Linköping, Sweden, 2008.

[4] V. Bansal, P. Poddar, A. Ahmad, and M. Sastry, "Room-temperature biosynthesis of ferroelectric barium titanate nanoparticles," *Journal of the American Chemical Society*, vol. 128, no. 36, pp. 11958–11963, 2006.

[5] M. S. Chavali and M. P. Nikolova, "Metal oxide nanoparticles and their applications in nanotechnology," *SN Applied Sciences*, vol. 1, Article ID 607, 2019.

[6] M. E. Franke, T. J. Koplin, and U. Simon, "Metal and metal oxide nanoparticles in chemiresistors," *Small*, vol. 2, no. 1, pp. 36–50, 2006.

[7] A. Haider, M. Ijaz, S. Ali et al., "Green synthesized phytochemically (*Zingiber officinale* and *Allium sativum*) reduced nickel oxide nanoparticles confirmed bactericidal and catalytic potential," *Nanoscale Research Letters*, vol. 15, Article ID 50, 2020.

[8] H. A. Salam and R. Sivaraj, "Green synthesis and characterization of zinc oxide nanoparticles from *Ocimum basilicum* L. var. *purpurascens* Benth.-Lamiaceae leaf extract," *Materials Letters*, vol. 131, pp. 16–18, 2014.

[9] G. Singhal, R. Bhavesh, K. Kasariya, A. R. Sharma, and R. P. Singh, "Biosynthesis of silver nanoparticles using *Ocimum sanctum* (Tulsi) leaf extract and screening its antimicrobial activity," *Journal of Nanoparticle Research*, vol. 13, pp. 2981–2988, 2011.

[10] C. Vidya, S. Hiremath, M. N. Chandraprabha et al., "Green synthesis of ZnO nanoparticles by *Calotropis gigantea*," *International Journal of Current Engineering and Technology*, vol. 1, no. 1, pp. 118–120, 2013.

[11] A. Kołodziejczak-radzimska and T. Jesionowski, "Zinc oxide—from synthesis to application: a review," *Materials*, vol. 7, no. 4, pp. 2833–2881, 2014.

[12] X. Wang, Y. Ding, C. J. Summers, and Z. L. Wang, "Large-scale synthesis of six-nanometer-wide ZnO nanobelts," *The Journal of Physical Chemistry B*, vol. 108, no. 26, pp. 8773–8777, 2004.

[13] D. B. Bharti and A. V. Bharati, "Synthesis of ZnO nanoparticles using a hydrothermal method and a study its optical activity," *Luminescence*, vol. 32, no. 3, pp. 317–320, 2017.

[14] B. M. Savi, L. Rodrigues, and A. M. Bernardin, "Synthesis of ZnO Nanoparticles by Sol−Gel Processing," Santa Catarina Extreme South University, pp. 1–8, 2011.

[15] H. Widiyandari, N. A. K. Umiati, and R. D. Herdianti, "Synthesis and photocatalytic property of zinc oxide (ZnO) fine particle using flame spray pyrolysis method," *Journal of Physics: Conference Series*, vol. 1025, Article ID 012004, 2018.

[16] K. L. Choy, "Chemical vapour deposition of coatings," *Progress in Materials Science*, vol. 48, no. 2, pp. 57–170, 2003.

[17] K. Yan, L. Fu, H. Peng, and Z. Liu, "Designed CVD growth of graphene via process engineering," *Accounts of Chemical Research*, vol. 46, no. 10, pp. 2263–2274, 2013.

[18] S. Dönmez, "Green synthesis of zinc oxide nanoparticles using *Zingiber officinale* root extract and their applications in glucose biosensor," *El-Cezeri Fen ve Mühendislik Dergisi*, vol. 7, no. 3, pp. 1191–1200, 2020.

[19] M. Naseer, U. Aslam, B. Khalid, and B. Chen, "Green route to synthesize zinc oxide nanoparticles using leaf extracts of *Cassia fistula* and *Melia azadarach* and their antibacterial potential," *Scientific Reports*, vol. 10, Article ID 9055, 2020.

[20] G. Von White, P. Kerscher, R. M. Brown et al., "Green synthesis of robust, biocompatible silver nanoparticles using garlic extract," *Journal of Nanomaterials*, vol. 2012, Article ID 730746, 12 pages, 2012.

[21] H. Mofid, M. S. Sadjadi, M. H Sadr, A. Banaei, and N. Farhadyar, "Green synthesis of zinc oxide nanoparticles using *Aloe vera* plant for investigation of antibacterial properties," *Advances in Nanochemistry*, vol. 2, no. 1, pp. 32–35, 2020.

[22] S. Abel, J. L. Tesfaye, R. Shanmugam et al., "Green synthesis and characterizations of zinc oxide (ZnO) nanoparticles using aqueous leaf extracts of coffee (*Coffea arabica*) and its application in environmental toxicity reduction," *Journal of Nanomaterials*, vol. 2021, Article ID 3413350, 6 pages, 2021.

[23] T. U. Doan Thi, T. T. Nguyen, Y. D. Thi, K. H. Ta Thi, B. T. Phan, and K. N. Pham, "Green synthesis of ZnO nanoparticles using orange fruit peel extract for antibacterial activities," *RSC Advances*, vol. 10, pp. 23899–23907, 2020.

[24] S. Pal, K. Pal, S. Mukherjee, D. Bera, P. Karmakar, and D. Sukhen, "Green cardamom mediated phytosynthesis of ZnONPs and validation of its antibacterial and anticancerous potential," *Materials Research Express*, vol. 7, Article ID 015068, 2020.

[25] M. G. Demissie, F. K. Sabir, G. D. Edossa, and B. A. Gonfa, "Synthesis of zinc oxide nanoparticles using leaf extract of *Lippia adoensis* (Koseret) and evaluation of its antibacterial activity," *Journal of Chemistry*, vol. 2020, Article ID 7459042, 9 pages, 2020.

[26] S. Banerjee, J. Banerjee, H. Mullick, and A. K. Ghosh, "*Zingiber officinale*: a natural gold," *International Journal of Pharma and Bio Sciences*, vol. 2, pp. 283–294, 2011.

[27] Y. Liu, J. Liu, and Y. Zhang, "Research progress on chemical constituents of *Zingiber officinale* Roscoe," *BioMed Research International*, vol. 2019, Article ID 5370823, 21 pages, 2019.

[28] M. Mahboubi, "*Zingiber officinale* Rosc. essential oil, a review on its composition and bioactivity," *Clinical Phytoscience*, vol. 5, Article ID 6, 2019.

[29] U. P. Singh, B. Prithiviraj, B. K. Sarma, M. Singh, and A. B. Ray, "Role of garlic (*Allium sativum* L.) in human and plant diseases," *Indian Journal of Experimental Biology*, vol. 39, no. 4, pp. 310–322, 2001.

[30] A. Haider, M. Ijaz, M. Imran et al., "Enhanced bactericidal action and dye degradation of spicy roots' extract-incorporated fine-tuned metal oxide nanoparticles," *Applied Nanoscience*, vol. 10, pp. 1095–1104, 2020.

[31] K. Dulta, G. K. Ağçeli, P. Chauhan, R. Jasrotia, and P. K. Chauhan, "A novel approach of synthesis zinc oxide nanoparticles by *Bergenia ciliata* rhizome extract: antibacterial and anticancer potential," *Journal of Inorganic and Organometallic Polymers and Materials*, vol. 31, pp. 180–190, 2021.

[32] S. Shaheen, A. Iqbal, M. Ikram et al., "Graphene oxide–ZnO nanorods for efficient dye degradation, antibacterial and in-silico analysis," *Applied Nanoscience*, vol. 12, pp. 165–177, 2022.

[33] M. Rashid, M. Ikram, A. Haider et al., "Photocatalytic, dye degradation, and bactericidal behavior of Cu-doped ZnO nanorods and their molecular docking analysis," *Dalton Transactions*, vol. 49, pp. 8314–8330, 2020.

[34] L. F. A. Raj, "Effect of zinc oxide nanoparticle produced by *Zingiber officinale* against pathogenic bacteria," *Journal of Chemical and Pharmaceutical Sciences*, vol. 8, no. 1, pp. 124–127, 2015.

[35] R. Yuvakkumar, J. Suresh, A. J. Nathanael, M. Sundrarajan, and S. I. Hong, "Novel green synthetic strategy to prepare ZnO nanocrystals using rambutan (*Nephelium lappaceum* L.) peel extract and its antibacterial applications," *Materials Science and Engineering: C*, vol. 41, pp. 17–27, 2014.

[36] M. Ikram, S. Aslam, A. Haider et al., "Doping of Mg on ZnO nanorods demonstrated improved photocatalytic degradation and antimicrobial potential with molecular docking analysis," *Nanoscale Research Letters*, vol. 16, Article ID 78, 2021.

[37] Manju, M. Jain, S. Madas et al., "Oxygen vacancies induced photoluminescence in $SrZnO_2$ nanophosphors probed by theoretical and experimental analysis," *Scientific Reports*, vol. 10, Article ID 17364, 2020.

[38] S. Alamdari, M. S. Ghamsari, C. Lee et al., "Preparation and characterization of zinc oxide nanoparticles using leaf extract of *Sambucus ebulus*," *Applied Sciences*, vol. 10, Article ID 3620, 2020.

[39] M. Khan, P. Ware, and N. Shimpi, "Synthesis of ZnO nanoparticles using peels of *Passiflora foetida* and study of its activity as an efficient catalyst for the degradation of hazardous organic dye," *SN Applied Sciences*, vol. 3, Article ID 528, 2021.

[40] P. Makuła, M. Pacia, and W. Macyk, "How to correctly determine the band gap energy of modified semiconductor photocatalysts based on UV–vis spectra," *The Journal of Physical Chemistry Letters*, vol. 9, no. 23, pp. 6814–6817, 2018.

[41] S. S. Kulkarni and M. D. Shirsat, "Optical and structural properties of zinc oxide nanoparticles," *International Journal of Advanced Research in Physical Science*, vol. 2, no. 1, pp. 14–18, 2015.

[42] M. F. A. Humánez, L. A. M. Vides, and O. A. Almanza-Montero, "Sol-gel synthesis of zinc oxide nanoparticle at three different temperatures and its characterization via XRD, IR and EPR," *DYNA*, vol. 83, no. 195, pp. 224–228, 2016.

[43] M. Ali, M. Ikram, M. Ijaz, A. Ul-Hamid, M. Avais, and A. A. Anjum, "Green synthesis and evaluation of n-type ZnO nanoparticles doped with plant extract for use as alternative antibacterials," *Applied Nanoscience*, vol. 10, pp. 3787–3803, 2020.

[44] B. Lallo da Silva, M. P. Abuçafy, E. Berbel Manaia et al., "Relationship between structure and antimicrobial activity of zinc oxide nanoparticles: an overview," *International Journal of Nanomedicine*, vol. 14, pp. 9395–9410, 2019.

[45] R. Dobrucka and J. Długaszewska, "Biosynthesis and antibacterial activity of ZnO nanoparticles using *Trifolium pratense* flower extract," *Saudi Journal of Biological Sciences*, vol. 23, no. 4, pp. 517–523, 2016.

[46] S. Umavathi, S. Mahboob, M. Govindarajan et al., "Green synthesis of ZnO nanoparticles for antimicrobial and vegetative growth applications: a novel approach for advancing efficient high quality health care to human wellbeing," *Saudi Journal of Biological Sciences*, vol. 28, no. 3, pp. 1808–1815, 2021.